agriculture

MDPI

Article

Parameter Optimization of Finger Clip Plate Garlic Seed-Metering Device

Yuangeng Ding [1,2], Hua Li [1,2,*], Jifeng Gao [1,2], Haiming Yu [1,2], Yongjian Wang [1,2] and Dinghao Feng [2,3]

[1] College of Engineering, Nanjing Agricultural University, Nanjing 210031, China; 2019112019@stu.njau.edu.cn (Y.D.); gjfnjnydx@163.com (J.G.); yuhaiming@njau.edu.cn (H.Y.); yjwang@njau.edu.cn (Y.W.)
[2] Key Laboratory of Intelligent Agricultural Equipment in Jiangsu Province, Nanjing 210031, China; dinghaofeng@njtech.edu.cn
[3] College of Mechanical and Power Engineering, Nanjing Tech University, Nanjing 211816, China
* Correspondence: lihua@njau.edu.cn

Abstract: In order to improve the success rate of garlic sowing and the qualification rate of garlic seeds, a fingerboard-type garlic seed metering device was designed, and its parameters were optimized. First, the structure and working principles of seed-metering devices were studied. Subsequently, its critical component parameters were determined using theoretical calculations; then, discrete element method multi-body dynamics (DEM-MBD)-coupling simulation software was used to explore the seed-metering device process and analyze the effects of the opening angle of the clamping plate, the diameter of the seed scoop, and rotational speed of the seeding plate on the single-seed rate, missing rate, and reply rate of the device. Finally, a quadratic regression orthogonal rotation simulation experiment was conducted using the splint opening angle, scoop opening diameter, and rotation speed of the seeding plate as experimental factors, with the single-seed filling rate, qualified percentage, and missing rate as evaluation indicators. A three-factor, five-level orthogonal test was conducted to determine the mathematical regression model of experiment factors and evaluation indicators and to realize parameter optimization. A bench validation test was conducted using a 63° splint opening angle, a 24 mm seed-collecting scoop opening diameter, and 34 r/min seed-metering plate rotation speed. The average qualified rate, missing rate, and reply rate of single seeds were 91.86%, 2.71%, and 5.43%, respectively, which was consistent with the regression model results. This indicates that the method proposed in this paper achieved parameter optimization of a fingerboard garlic seed metering device.

Keywords: garlic; finger clip type; seed-metering device; opening angle of the splint; bench test

check for updates

Citation: Ding, Y.; Li, H.; Gao, J.; Yu, H.; Wang, Y.; Feng, D. Parameter Optimization of Finger Clip Plate Garlic Seed-Metering Device. *Agriculture* **2023**, *13*, 2071. https://doi.org/10.3390/agriculture13112071

Received: 2 October 2023
Revised: 17 October 2023
Accepted: 24 October 2023
Published: 28 October 2023

Copyright: © 2023 by the authors. Licensee MDPI, Basel, Switzerland. This article is an open access article distributed under the terms and conditions of the Creative Commons Attribution (CC BY) license (https://creativecommons.org/licenses/by/4.0/).

1. Introduction

Mechanized seeding is an integral part of mechanized garlic production. Seed meters are a critical part of the seeding machine, the performance of which is crucial for determining the quality of the garlic mechanical seeding process. However, owing to large particle sizes, irregular shapes, and the rough surface of garlic seeds, it can be easy to reply or miss seeds in the seeding process [1–3]. Therefore, the study of single-seed extraction technology for garlic seed-metering devices is essential. The fingerboard-type garlic seed metering device can accurately measure garlic seeds, which is a key link to ensure the quality and efficiency of agricultural production and plays an important role in improving agricultural production efficiency and farmers' income. The fingerboard-type garlic seed metering device can improve the accuracy and efficiency of seed metering, reduce the cost and error of manual operation, and also improve the utilization rate of seeds, and reduce waste. This study can also promote the development of agricultural mechanization and intelligence, improving the automation level and production efficiency of agricultural

production. Therefore, research on the fingerboard garlic seed metering device is of great significance in promoting agricultural modernization and sustainable development.

Currently, seed-metering devices for large seeds, such as garlic, include the spoon belt, cell feed wheel, socket wheel, spoon chain, rotary spoon, finger clip plate, as well as vibrating-type devices [4–7]. The socket wheel type is simple in structure and low in cost, but seeds can become struck easily because of the irregular morphology of garlic seeds. Regarding the spoon chain type, it can be easily affected by the vibration of the machine, and missing seeds are common. Pneumatic meters have good seeding quality and high efficiency, but their structure is complex, and their size and power consumption are considerable [8]. The finger clip plate type seed-metering device uses the tension of the return spring to clip seeds, which has the advantage of a simple structure and good adaptability to seeds' size, shape, and working speed. It is widely used in precision seeding crops with tiny particle-sized seeds [9–11]. However, relevant research on garlic finger clip plate-type seed-metering devices lacks depth.

Zhang Jiao et al. proposed a design method for the key components of garlic seeders [12], using adjustable containers or trays to arrange the spacing of garlic seeds and feed them into the planting slots one by one. The planting trough is the storage and transmission channel for seeds, which needs to have good guidance and an appropriate depth to ensure normal seed sowing. When designing, consideration should be given to the characteristics of garlic seeds, such as shape, size, and vertical arrangement, to ensure that each seed can correctly fall into the sowing row. The spacing between garlic planting rows is determined based on specific needs, and the seeder needs to have corresponding mechanisms to adjust spacing according to planting needs. The seeder needs a stable and smooth motion mechanism to ensure the stability and continuity of the entire planting process. Usually, transmission devices that connect rods and motion shafts are used to achieve the movement of the seeder. The seeder also needs to have corresponding control systems to monitor and control parameters such as sowing speed, density, and depth. The control system can use sensors and electronic control devices to achieve an automated seeding process. Finally, the design of key components should comprehensively consider factors such as the characteristics of garlic seeds, sowing requirements, and the convenience and efficiency of the operation in order to improve the planting effect and work efficiency of garlic seeders. This method can effectively improve the sowing speed, but the reply rate costs are high.

In response to the problem of a high reply rate in the above methods, this paper designs a parameter optimization method for a fingerboard garlic seed metering device, using a combination of the discrete element method (DEM) and multi-body dynamics (MBD) analysis method. At present, DEM-MBD-coupled simulation technology has been widely applied in the field of agricultural engineering [13,14]. Therefore, a DEM-MBD-coupled simulation model was established for finger clamp seed measuring instruments to explore the motion state of garlic seeds and improve the performance of this type of seed measuring instrument.

With white garlic from Pizhou in China's Jiangsu as the research target and exploiting the design concepts from former studies in the literature, we investigated a finger clip plate-type seed meter that could perform the seeding process by controlling the opening and closing of the splint. In the present study, a 3D model was developed in the case of the proposed seed meter, and subsequently, a theoretical assessment proceeded on the vital component variables. The relevant parameters of the seed feeder's critical components were then determined and optimized based on a single-factor simulation test and a 3-factor 5-level simulation, adopting the quadratic regression orthogonal rotation combination design. In addition, optimized outcomes were verified through bench tests, providing considerable data support when optimizing the design of garlic seed meters.

2. Materials and Methods

2.1. Structure of Seed-Metering Device

The proposed finger clip disc seed meter for garlic comprises a seed-metering plate, splints, a seed-collecting scoop, a fine adjustment spring, soft leather, a rotation shaft, a falling seed guide, and plates, as shown in Figure 1.

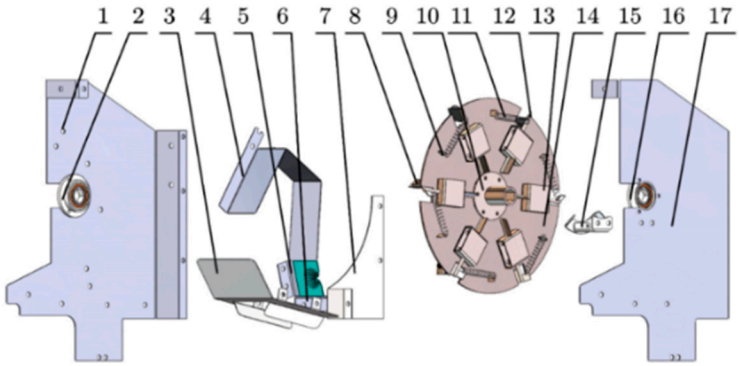
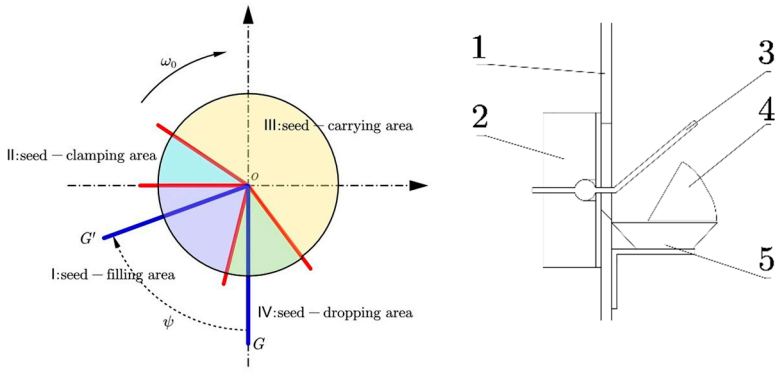


Figure 1. Plot of proposed seed meter: 1. Left-side plate; 2. Bearing; 3. Falling velocity guide; 4. Front plate of the seed box; 5. Soft leather; 6. Bottom plate of seed box; 7. Right plate of seed box; 8. The seed-collecting scoop; 9. The fixator of the fine adjustment spring; 10. The rotation shaft; 11. The fine adjustment spring; 12. The splint; 13. The fixator of the splint; 14. The seed-metering plate; 15. Control board for seed opening and closing; 16. The bearing; 17. The right-side plate.

2.2. Working Principle of Seed-Metering Device

As displayed in Figure 2a, there are four areas in the designed finger clip plate seed meter for garlic, i.e., a seed-filling area (I), a seed-clamping area (II), a seed-carrying area (III), as well as a seed-dropping area (IV).



(**a**) (**b**)

Figure 2. Plot the working principle of the seed meter. (**a**) Schematic of the work area; (**b**) Schematic of seed-carrying process; 1. Seed-metering plate; 2. Splint fixator; 3. The splint; 4. Garlic seeds; 5. Seed-collecting scoop.

With the proposed seed meter in operation, garlic seeds were fed into the seed box's seed-filling area via gravity and the forces between the seeds while the seed-metering plate rotated with the meter's rotation shaft. The splint's opening and closing were controlled via the coordination of a seed opening and closing control board along with the fine adjustment spring.

Figure 2b illustrates the seed-filling principle. During the entry of the seed-collecting scoop and splint into the seed-filling area, the splint caudal plate enters the control board for seed opening and closing, and the state of the splint is open. The garlic seeds in the seed box's seed-filling area are disturbed by the seed-collecting scoop and splint, which disrupts

the steady seed state so that the area formed by the seed-collecting scoop and splint is filled with garlic seeds. When the seed-collecting scoop and splint enter the seed-clamping area, the splint remains closed and clamped. Through the actions of garlic seeds' gravity and splint force, unstable and clamped excess garlic returns to the seed box. The seed-collecting scoop and splint securely clamp the remaining single garlic seed into the seed-carrying area. Here, the splint is closed using the force of the fine adjustment spring, and the single garlic seed in the clamping area is clamped tightly to finish the seed-carrying process. When the seed-collecting scoop and splint enter the seed-dropping area, the caudal plate of the splint drives the splint to open. The single garlic seed in the clamping area is no longer affected by the clamping force from the fine adjustment of the spring and falls to the seed furrow via gravity, thereby finishing the seed-dropping process.

2.3. Design of Seed-Collecting Scoop

The seed-collecting scoop, as a critical seed meter element, achieves seed isolation from the seed box, as well as seed clamping with a splint [15]. In order to increase the scoop surface–seed contact area, prevent garlic from being pushed out of the clamping area during the clamping process, and ensure that garlic seeds can be clamped in the filling process, the seed scoop is designed as a circular, truncated cone shape, as shown in Figure 3. Its main structural parameters are the diameter (R) of the seed-collecting scoop, its depth (H), and angle (θ).

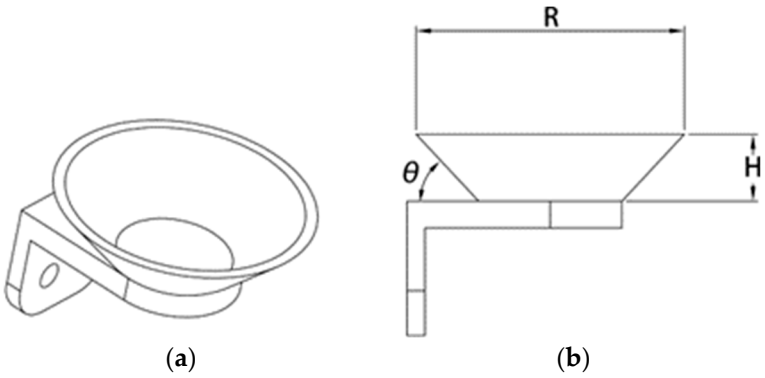


Figure 3. Structural diagram of the seed-collecting scoop. (**a**) 3D view of the seed-collecting scoop; (**b**) Front view for seed-collector scoop.

Regarding the design of the seed-collector scoop, the intra-scoop garlic state and the three-dimensional size of the seeds should be considered. Consequently, 100 full white garlic seeds from Pizhou were randomly selected as the objects for triaxial size measurements, as displayed in Table 1.

Table 1. Three-dimensional size of the seeds.

Physical Parameters	Maximum	Minimum	Average
Length of garlic (mm)	36.48	24.09	30.34
Height of garlic (mm)	24.19	13.52	18.62
Thickness of garlic (mm)	24.51	14.36	18.54

Based on Figure 4, the posture of garlic seeds entering the collector scoop can be divided into three positions—side-lying, lying, and standing postures. The distribution probability can be calculated as 39.82% for the side-lying posture, 42.94% for the lying posture, and 17.24% for the standing posture when the garlic seed enters the seed-collecting scoop. Therefore, based on the concept of minimum potential energy [16,17], the side-lying and lying postures were used for seed-collecting scoop size design principles.

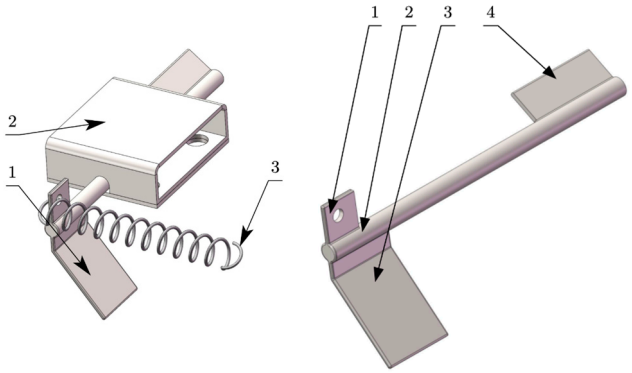


Figure 4. Schematic illustration for clamping mechanism. (**a**) Clamping mechanism schematization; 1. The splint; 2. The fixator of the splint; 3. The fine adjustment spring. (**b**) Schematic diagram of the splint; 1. The holder of the fine adjustment spring; 2. The splint rotation shaft; 3. The splint; 4. The caudal plate of the splint.

In terms of the length, in order to guarantee that side-lying or lying is the posture of a single garlic seed entering the seed-collector scoop, the opening diameter (D) of the scoop must exceed the mean garlic seed width (W_0) and be less than its average length (L_0). In the depth direction, for the intra-scoop seed barycenter of garlic, the scoop depth (H) must exceed half of the mean thickness of the garlic seed (T_0) and fall below half of its mean length (L_0). For the seed-collector scoop to be a circular truncated cone shape, it is necessary for its bottom diameter to exceed half of its opening diameter. Consequently, the scoop's structural variables need to satisfy the criteria shown below:

$$\begin{cases} w_0 < D < l_0 \\ \frac{h_0}{2} < H < \frac{l_0}{2} \\ D - \frac{2H}{\tan\theta} > \frac{D}{2} \end{cases} \quad (1)$$

Based on the above formula, the seed-collecting scoop has opening diameters varying between 20 and 28 mm. If the scoop diameter is extremely large, it increases the reply rate under the condition that the seed meter is working; an excessively small diameter likely leads to missing seeds. Therefore, the shovel depth (H) can be 10–14 mm, with angle (θ) of the seed-collecting scoop at 60°. According to the pre-experiment and based on the principle of reducing the cost of the test, the shovel depth (H) was finally taken as 10 mm.

2.4. Design of Clamping Mechanism

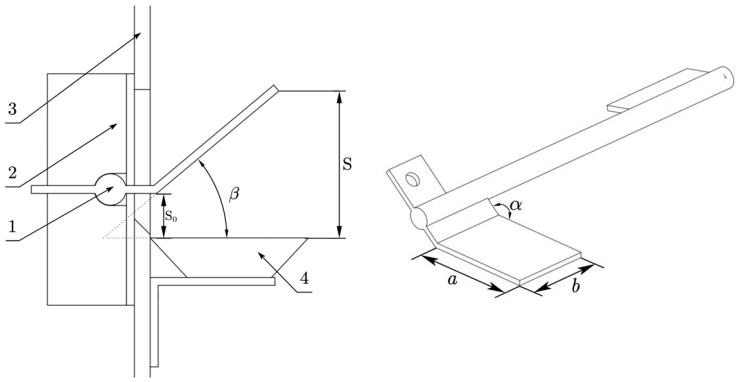
The clamping mechanism is one of the critical components for the finger clip plate-type seed meter of garlic. It comprises a splint, a fine adjustment spring, and the fixator of the splint, as shown in Figure 4. A bolt is used to fix the fixator of the splint to the seed-metering plate, and the splint can rotate for the plate. Both sides of the fine adjustment spring are connected to the plate holder as well as the splint holder.

In the process of filling the seed, a certain angle is formed between the splint and seed-collector scoop, which is called the splint-opening angle (β), as depicted in Figure 5. The splint-opening angle (β) is controlled by the length of the splint tailpiece and the splint bending angle (α), as shown in Figure 5. The primary structural parameters of the splint include the splint length (a) and splint width (b). To improve the stability of the splint's clamping performance, both the splint's length and width must exceed the maximum garlic seed width and thickness. The splint length (a) and splint width (b) can be determined as 25 mm. In order to guarantee that the garlic seeds can enter the clamping area smoothly

when the splint is open, the distance (S) from the top of the scoop to the bottom must be beyond the maximum garlic seed thickness and width. It can be calculated as follows:

$$S = a\sin\beta + S_0 \tag{2}$$

where S_0 denotes the minimum distance from the splint to the seed-collecting scoop. For the purposes of Equation (2), the minimum splint opening angle (β) is 40°. If the splint opening angle (β) is too great, multiple garlic seeds simultaneously enter the area between the splint and the scoop, increasing the reply rate. If it is too small, the area between the splint and the scoop is reduced, and the possibility of no seed entering the scoop increases. Therefore, it is necessary to determine the splint opening angle using a simulation test.

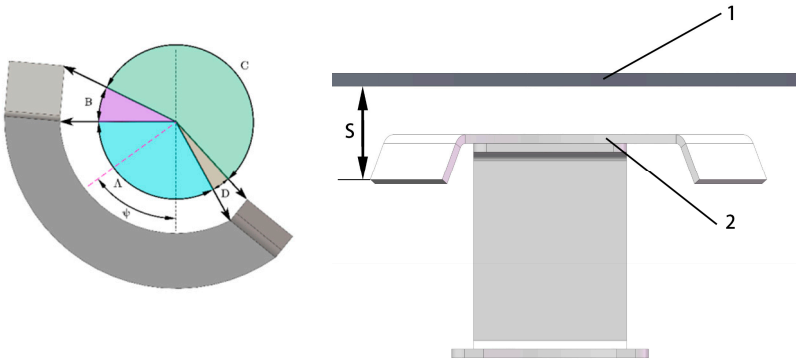


(**a**) (**b**)

Figure 5. Schematization for the clamping mechanism's structural parameters; (**a**) The splint opening angle; 1. The splint; 2. The fixator of the splint; 3. Seed-metering plate; 4. Seed-collector scoop; (**b**) Structural parameters of the splint.

2.5. Seed Opening and Closing Control Board

The control board controls the opening along with the closing of the clamping mechanism. It is a critical seed meter controller component designed to ensure the functional implementation of the meter device, as illustrated in Figure 6a.



(**a**) (**b**)

Figure 6. Schematic diagram of the control board for seed opening and closing; (**a**) Partition chart of the control board; (**b**) Distance between the control board and seed-metering plate.1. The seed-metering plate.2. The control board.

Based on Figure 6a, the control board was designed with four areas, namely the splint opening fully area (A), the splint closing gradually area (B), the splint closing fully area (C), and the splint opening gradually area (D). When the location of the splint is in the opening fully area, a fixed-sized clamping area is formed between the splint and the seed-collecting scoop. To ensure the clamping area fills a single garlic seed smoothly, the angle of the splint

opening fully area should be increased as much as possible. When the splint is in the splint closing gradually area, the splint should be progressively closed to lower the effect of the splint on the garlic seed. When the splint is in the splint closing fully area, it is unaffected by the control board. To ensure that garlic seeds can be dropped from the clamping area in the same position after the splint enters the opening gradually area, the opening time of the cleat in the seeding process should be shortened.

Figure 6b depicts the schematic diagram of the distance (S) between the control board and the seed-metering plate. Based on the foregoing design concepts in conjunction with the working process analysis, the relationship of the distance (S) between the control board and seed-metering plate with the phase angle (ψ) is expressible as follows:

$$S = \begin{cases} 14 + 5 \times \frac{(325^\circ - \psi)}{15^\circ} (310^\circ \leq \psi < 325^\circ) \\ 14 (325^\circ \leq \psi < 360^\circ, 0^\circ \leq \psi < 90^\circ) \\ 14 + 5 \times \frac{\delta - 90^\circ}{30^\circ} (90^\circ \leq \psi \leq 120^\circ) \end{cases} \quad (3)$$

2.6. Design of Seed-Metering Plate

For the seed-metering plate, its critical parameters include the plate itself, as well as the quantity of seed-collector scoops. A larger plate diameter means a higher scoop quantity and lower seed tray angular speed, which makes the seed filling more stable. However, it increases the seed-metering plate's size and power consumption. Given the size of garlic seeds, along with the holistic architecture and component distribution of the seed platter, the seed-metering plate's diameter is 320 mm. In accordance with the literature [10], to guarantee that the garlic seed distance does not change with the speed of the planter, the following relationship is satisfied:

$$\frac{s}{2\pi} = \frac{\omega_m R_m}{\omega t} \quad (4)$$

where s denotes the garlic seed distance, ω_m denotes the wheel rotation angular velocity, ω denotes the seed-metering plate rotation angular velocity, R_m denotes the earth wheel radius, and t denotes the number of seed-collector scoops. Conforming to the agronomic demands of Pizhou-sourced white garlic, the garlic seed distance was 13–18 cm, and the number of seed scoops was 6.

2.7. DEM-MBD-Coupling Simulation

During the operational process of the finger clip plate-type seed meter for garlic, the contact collisions between the seeds themselves, between seeds and parts of the seed meter, as well as splint opening and closing during the operation, cannot be simulated by a single software application alone. Consequently, the DEM-MBD-coupling simulation method was applied in this study concerning the finger clip plate-type seed meter.

2.7.1. MBD Model Development

It is possible to simulate the rotation and opening of the splints in the proposed seed meter through the application of RecurDyn MBD software. First, the model is built in 3D modeling software, after which the model can be converted into an X_T format and imported into RecurDyn for MBD simulation, as displayed in Figure 7. Here, we set the seed meter model and density separately to steel and 7.8 g/cm^3.

During the operation of the proposed seed meter, the seed-metering axle drove the rotation of the seed-metering plate, which drove the seed-collecting scoop and splint to complete seed-metering functions. As a result, it is necessary to add constraints between each component in RecurDyn, the main constraints being the rotation pair with the ground as the reference frame, a fixed pair added to the seed box and control board for seed opening and closing with the ground as the reference system, solid-to-solid contact added between each splint, the seed-metering plate and the control board, respectively, as well as a rotating pair added between each splint and the seed-metering plate.

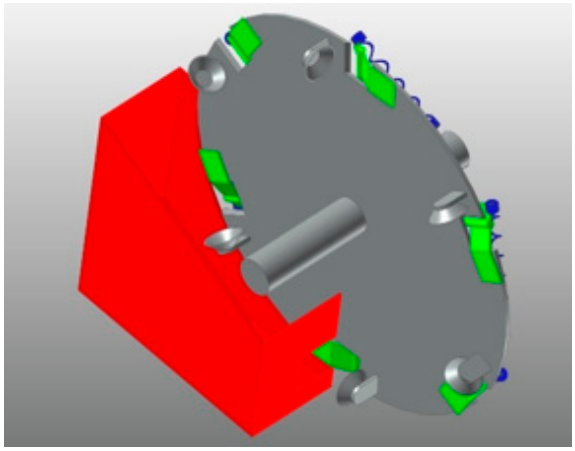
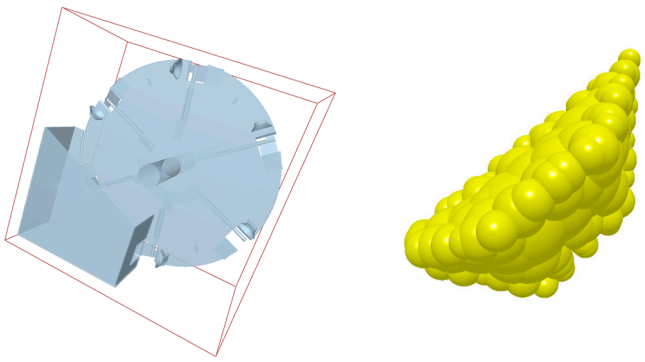


Figure 7. Seed-metering device model in RecurDyn.

Based on the simulation test requirements, the corresponding rotation speed can be added to the seed plate rotational pair. For the opening and closing control over the splint via the spring force, a spring module can be added between each splint and the corresponding holder of the fine adjustment spring, with the fine adjustment spring parameters (such as spring stiffness coefficient, damping coefficient, free length, and existing length) added. Among these, the spring stiffness coefficient of the garlic seed metering device is 600 N/m, the damping coefficient is 0.8 Ns/m, the free length is 8 cm, and the existing length is 11 cm.

2.7.2. Establishment of DEM Model

Under the coupling interface between the discrete element software application (EDEM) and RecurDyn, the external SPI module in RecurDyn can be exploited to export the established seed meter model in a wall file form, after which the meter model file is imported and generated into EDEM, as displayed in Figure 8a.



(**a**) (**b**)

Figure 8. Models in EDEM. (**a**) Seed meter model in EDEM; (**b**) DEM model for garlic seeds.

The particle model used in the simulation was Pizhou-sourced white garlic seed. The 3D seed particle model was developed and input into EDEM. The rapid particle filling function was employed to acquire the multi-spherical polymer seed particle model, as displayed in Figure 8b.

In the discrete element model (DEM), three-dimensional coordinate data of the seed surface are obtained through laser scanning, and then the geometric model of the seed is constructed. The determination of model parameters usually requires experimental measurement and calibration. Physical experiments or numerical simulations are conducted on garlic seeds to obtain parameters such as mechanical properties and motion characteristics

under different conditions. The elastic modulus of garlic seeds is taken as 5.6 GPa, the friction coefficient is taken as 0.5, and the rolling resistance coefficient is taken as 0.1. Then, these parameters are input into the DEM model for calculation and simulation.

The contact models of particle–particle and particle–geometry models were both Hertz–Mindlin non-slip models [3], while the parts of the seed meter in contact with garlic seeds were 45 steel. After parameter determination, the material and mechanical properties of the garlic seeds and steel were the same as those presented in Table 2, and the simulation results are displayed in Figure 9 [15].

Table 2. Simulation parameters.

Parameter	Garlic Seed	45 Steel
Poisson's ratio	0.28	0.30
Shear modulus (MPa)	1×10^8	7×10^{10}
Density (g/cm^3)	7.8	7.800
Collision recovery factor	0.487	0.503
Static friction factor	0.511	0.503
Rolling friction factor	0.108	0.111

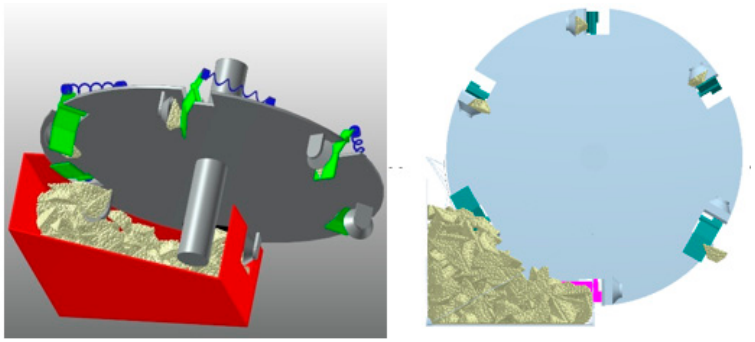


Figure 9. Coupled simulation work processes.

3. Simulation Results and Discussion

3.1. DEM-MBD-Coupling Simulation

To achieve design optimization for the proposed finger clip plate-type seed meter for garlic, a univariate simulation test was conducted through DEM-MBD coupling. According to the pre-test, the primary influencing factors of seed meter efficiency included the splint opening angle, seed-collecting scoop opening diameter, and seed-metering plate rotation speed. Through a theoretical calculation, combined with the research findings of the existing finger clip seed dispenser, it was evident that the splint opening angle was within a 40–80° scope, the scoop opening diameter was within the range of 20–28 mm, and the plate rotational velocity was within a 10–50 rpm scope. Consequently, a univariate simulation test was performed, and Table 3 displays the experimental scheme. During the experiment, 100 seed-collecting scoops were counted, with the experiment repeated five times for each group.

Table 3. Single-factor experiment scheme.

Factor Levels	Splint Opening Angle (°)	Scoop Opening Diameter (mm)	Plate Rotation Speed (rpm)
1	40	20	10
2	50	22	20
3	60	24	30
4	70	26	40
5	80	28	50

In the simulation test, the rates of single-seed eligibility (Y_1), reply (Y_2), and missing (Y_3) were chosen as test indices to assess the seed meter operating performance. Then, the formula for each test index could be expressed as follows:

$$\begin{cases} Y_1 = \frac{n_1}{n} \times 100\% \\ Y_2 = \frac{n_2}{n} \times 100\% \\ Y_3 = \frac{n_3}{n} \times 100\% \end{cases} \quad (5)$$

where n_1 represents the number of garlic seeds that meet the quality standards; n_2 represents the number of garlic seeds that failed to successfully sow into the soil; and n_3 represents sowing garlic seeds multiple times on the same plot, where n represents the total number of garlic seeds. The qualification rate Y_1 of garlic seeds refers to the proportion of garlic seeds that meet quality standards after testing and screening, usually expressed as a percentage. This indicator reflects the quality and purity of seeds and is of great significance for ensuring the smooth progress of agricultural production.

The missed sowing rate Y_2 of garlic seeds refers to the proportion of garlic seeds that were not successfully sown into the soil during the sowing process. Missing seeds can affect the emergence rate and yield of farmland, so reducing the missing seeding rate is an important link to improve agricultural production efficiency.

The reply sowing rate Y_3 of garlic seeds refers to the proportion of garlic seeds sown multiple times on the same plot. Reply sowing can lead to seed waste and the excessive density of farmland, affecting seed growth and development, so it is also necessary to avoid it as much as possible.

3.2. Influence of Different Factors on Working Performance

3.2.1. Splint Opening Angle

The scoop opening diameter was assigned 24 mm, the rotational velocity of the seed-metering plate was assigned 30 rpm, and the splint opening angles were set to 40°, 50°, 60°, 70°, and 80°, respectively, for the DEM-MBD-coupling simulation purpose. Figure 10 displays the test result analyses. With the splint opening angle gradually growing, the missing rate exhibited a monotonically decreasing trend, the reply rate exhibited a monotonically increasing trend, and the qualified rate first increased before decreasing. The qualified rate reached its maximum when the splint opening angle was 60°. When the splint opening angle was between 50° and 70°, the seed plate exhibited superior operating performance, with a qualified rate of above 80%.

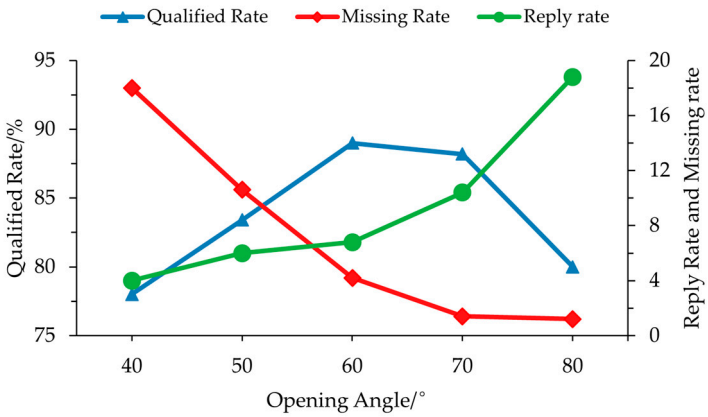


Figure 10. Effect of the splint opening angle on the test indices.

3.2.2. Plate Rotation Speed

During the DEM-MBD-coupling simulation, the scoop opening diameter and splint opening angle were assigned separately at 24 mm and 60°, while the plate rotation velocities were 10, 20, 30, 40, and 50 rpm, respectively. Figure 11 presents the outcome of the test

analyses. The eligible single-seed proportion increases with the plate rotation speed before decreasing after reaching its maximum value at 40 rpm. When the rotation velocity of the plate was below 30 rpm, it made no significant impact on the missing rate. With the plate rotation speed greater than 30 rpm, the missing rate increased significantly with increasing plate rotation speed. The reply rate decreased with an increasing plate rotation speed, and the reply rate remained unchanged when the plate rotation speed exceeded 40 rpm. In this case, the rotation velocity of the plate is within a 20–40 rpm scope, while a higher qualified proportion, lower missing and reply rates, as well as the superior operating performance of the seed meter are attainable.

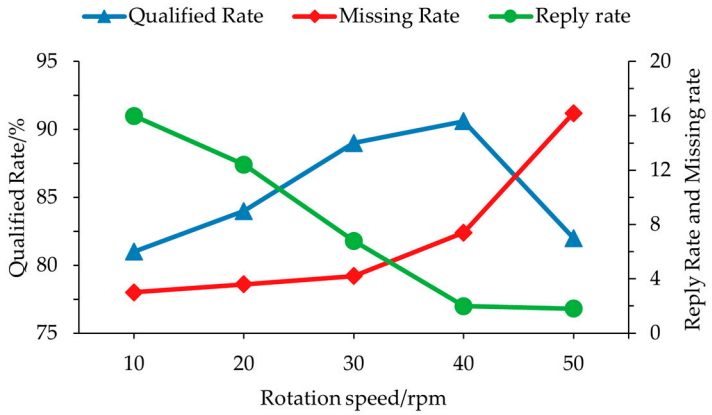


Figure 11. Impact of seed-metering plate's rotation velocity on test indices.

3.2.3. Diameter of Seed-Collecting Scoop

The splint opening angle was set at 60°, while the seed-metering plate's rotation velocity was assigned 30 rpm. To implement the DEM-MBD-coupling simulation, five diameters were selected for the seed-collector scoop—that is, 20, 22, 24, 26, and 28 mm. Figure 12 shows the analysis of the test results. With the increasing scoop diameter, there was a monotonic decline in the missing rate, as well as a monotonic elevation in the reply rate. At a 24 mm scoop diameter, the eligible single-seed proportion reached its maximum. When the scoop diameter varied between 22 and 26 mm, a higher qualified single-seed proportion, lower missing and reply rates, as well as the superior operating performance of the seed meter were attainable.

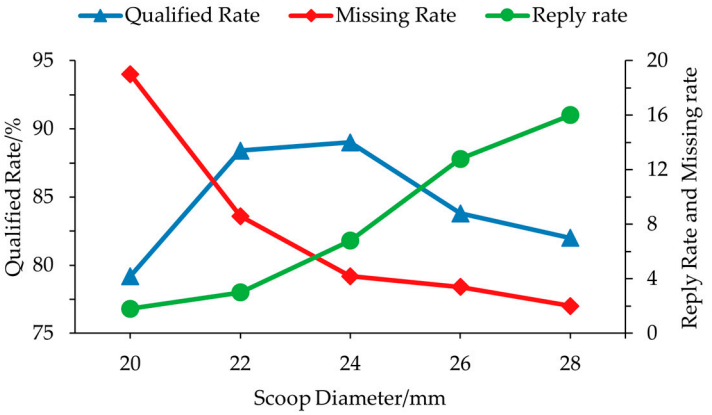


Figure 12. Effect of the diameter of the seed-collecting scoop on test indices.

3.3. Quadratic Regression Orthogonal Rotation Combination Simulation Test

During the univariate test, the impacts of the splint opening angle, plate rotation speed, and scoop opening diameter on the performance indicators of the seed meter were obtained. However, there could still be an interplay among the influencing variables of the seed meter operating performance. To study the interplay among the three foregoing

factors, the corresponding mathematical model was established, followed by the selection of an optimal variable combination. It became necessary to conduct a simulation test by adopting a quadratic regression orthogonal rotation combination design. Table 4 displays the univariate test-based coding details.

Table 4. Factor levels of the quadratic regression orthogonal rotation combination simulation test.

Factor Levels	Splint Opening Angle (X_1) (°)	Scoop Diameter (X_2) (mm)	Plate Rotation Speed (X_3) (rpm)
−1.682	50.00	22.00	20.00
−1	54.05	22.81	24.05
0	60.00	24.00	30.00
1	65.95	25.19	35.95
1.682	70.00	26.00	40.00

Using the splint opening angle (X_1), scoop opening diameter (X_2), and plate rotation speed (X_3) as test factors and using the qualified rate of the single-seed, reply rate, and missing rate as test indicators, a quadratic regression orthogonal rotation combination simulation test with three factors and five levels was performed to investigate the influence of interactions between different parameters on the test indicators of the seed-metering device. Based on an analysis of the single-factor simulation test, the scoop opening diameter was selected to be 22–26 mm, the splint opening angle was 50–70°, and the plate rotation speed was 20–40 rpm in the multi-factor test. Table 5 shows factors and levels of the multi-factor test.

Table 5. Factors and levels of the multi-factor test.

No.	Experimental Factors			Qualified Rate Y_1 (%)	Missing Rate Y_2 (%)	Reply Rate Y_3 (%)
	X_1	X_2	X_3			
1	−1	−1	−1	85.8	7.6	6.6
2	1	−1	−1	87.4	2.6	10
3	−1	1	−1	79.4	7.2	13.4
4	1	1	−1	82	2.2	15.8
5	−1	−1	−1	87.2	11.6	1.2
6	1	−1	−1	85.4	8	6.6
7	−1	1	−1	85.4	8.4	6.2
8	1	1	−1	88.6	1.8	9.6
9	−1.682	0	0	83.4	10.4	6.0
10	1.682	0	0	89.0	1.2	9.8
11	0	−1.682	0	88.4	8.6	3.0
12	0	1.682	0	83.8	3.4	12.8
13	0	0	−1.682	82.8	3.6	13.6
14	0	0	1.682	90.6	7.4	2.0
15	0	0	0	89.4	4.8	5.8
16	0	0	0	90.4	4.8	4.8
17	0	0	0	89.4	3.8	6.8
18	0	0	0	88.0	5.0	7.0
19	0	0	0	90.0	3.4	6.6
20	0	0	0	90.0	4.4	5.6

Table 6 shows the variance analysis of the regression model. Design-Expert software was used to complete the multiple regression fitting analysis of the test data [18–21], and

the quadratic multiple regression equation for the qualified rate of single-seed, missing rate, reply rate, and three factors were obtained as follows:

$$\begin{cases} Y_1 = & 89.57 + 1.10X_1 - 1.33X_2 + 1.84X_3 + 0.75X_1X_2 - 0.35X_1X_3 \\ & +1.65X_2X_3 - 1.39X_1^2 - 1.42X_2^2 - 1.21X_3^2 \\ Y_2 = & 4.36 - 2.61X_1 - 1.39X_2 + 1.21X_3 - 0.38X_1X_2 - 0.03X_1X_3 \\ & -1.07X_2X_3 + 0.58X_1^2 + 0.65X_2^2 + 0.47X_3^2 \\ Y_3 = & 6.08 + 1.54X_1 + 2.72X_2 - 3.05X_3 - 0.38X_1X_2 + 0.38X_1X_3 \\ & -0.58X_2X_3 + 0.78X_1^2 + 0.78X_2^2 + 0.75X_3^2 \end{cases} \quad (6)$$

Table 6. Variance analysis of regression model.

Size Levels	Source	Sum of Squares	df	F Value	*p* Value
Qualified rate of single-seed	Model	179.25	9	14.2	0.0001
	X_1	16.51	1	11.78	0.0064
	X_2	24.08	1	17.18	0.002
	X_3	42.2	1	32.95	0.0002
	$X_{1\times2}$	4.5	1	3.21	0.1035
	$X_{1\times3}$	0.98	1	0.6989	0.4227
	X_2X_3	21.78	1	15.53	0.0028
	${X_1}^2$	27.73	1	19.78	0.0012
	${X_2}^2$	29.17	1	20.8	0.001
	${X_3}^2$	21.12	1	15.06	0.0031
	Residual	14.02	10		
	Lack of fit	10.45	5	2.92	0.132
	Pure error	3.57	5		
	Cor total	193.27	19		
Missing rate	Model	161.69	9	45.46	<0.0001
	X_1	93.18	1	235.78	<0.0001
	X_2	26.28	1	66.5	<0.0001
	X_3	20.16	1	51	<0.0001
	X_1X_2	1.13	1	2.85	0.1225
	X_1X_3	0.005	1	0.0127	0.9127
	X_2X_3	9.25	1	23.39	0.0007
	${X_1}^2$	4.76	1	12.06	0.006
	${X_2}^2$	6.01	1	15.2	0.003
	${X_3}^2$	3.17	1	8.02	0.0178
	Residual	3.95	10		
	Lack of fit	1.92	5	0.9436	0.5246
	Pure error	2.03	5		
	Cor total	165.64	19		
Reply rate	Model	286.77	9	36.37	<0.0001
	X_1	32.26	1	36.83	0.0001
	X_2	100.69	1	114.93	<0.0001
	X_3	127.38	1	145.4	<0.0001
	X_1X_2	1.13	1	1.28	0.2836
	X_1X_3	1.13	1	1.28	0.2836
	X_2X_3	2.64	1	3.02	0.1129
	${X_1}^2$	8.87	1	10.12	0.0098
	${X_2}^2$	8.87	1	10.12	0.0098
	${X_3}^2$	8.08	1	9.23	0.0125
	Residual	8.76	10		
	Lack of fit	5.18	5	1.45	0.3475
	Pure error	3.58	5		
	Cor total	295.53	19		

In the regression equation for the qualified rate, the p values of X_1X_3 and X_1X_2 were all greater than 0.05, so their effects on the qualified rate of single-seed were not significant, while other items had significant effects on the qualified rate of single-seed. In the regression equation for the missing rate, the p values of the interaction terms X_1X_3 and X_1X_2 were all greater than 0.05, so their effects on the missing rate were not significant, while other items had significant or extremely significant effects on the missing rate. In the regression equation for the reply rate, the p values of interaction terms X_2X_3, X_1X_3, and X_1X_2 were all greater than 0.05, so their effects on the reply rate were not significant, while other items had significant or extremely significant effects on the reply rate. Additionally, in the above regression equation, missing fitting terms were not significant, suggesting that no other major factors were influential.

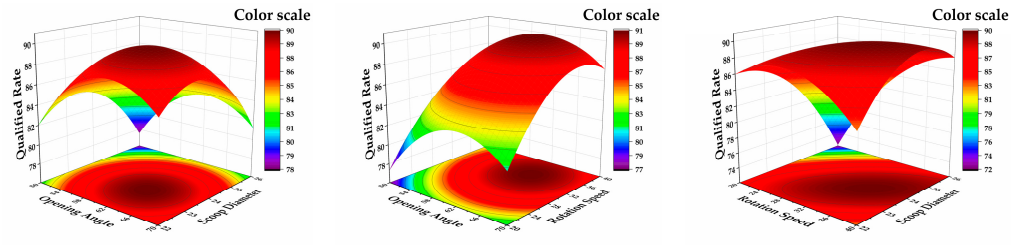
After the elimination of non-significant factors, the regression equations for the qualified rate of single-seed, the missing seeding rate, and the reply rate were re-fitted, the regression equations were obtained as shown in Equation (7). The three regression equations were tested, and the main and secondary factors affecting the qualified rate were found to be the plate rotation speed, scoop opening diameter, and splint opening angle. The main and secondary factors affecting the missing rate were found to be the splint opening angle, scoop opening diameter, and plate rotation speed. The main and secondary factors affecting the reply rate were found to be the plate rotation speed, scoop opening diameter, and splint opening angle.

$$\begin{cases} Y_1 = 89.57 + 1.10X_1 - 1.33X_2 + 1.84X_3 + 1.65X_2X_3 - 1.39X_1^2 - 1.42X_2^2 - 1.21X_3^2 \\ Y_2 = 4.36 - 2.61X_1 - 1.39X_2 + 1.21X_3 - 1.07X_2X_3 + 0.58X_1^2 + 0.65X_2^2 + 0.47X_3^2 \\ Y_3 = 6.08 + 1.54X_1 + 2.72X_2 - 3.05X_3 + 0.78X_1^2 + 0.78X_2^2 + 0.75X_3^2 \end{cases} \quad (7)$$

3.4. Each Factor Interaction Influence Analysis and Parameter Optimization

After the use of Design-Expert 13.0 software to explore data in the previous section, the influence of the splint opening angle, scoop opening diameter, and seed-metering plate rotation speed on the test index of the seed-metering device was obtained. The interactive influence of test factors was analyzed by drawing the response surface diagram [22].

Figure 13a presents the response surface diagram for the interaction between the scoop opening diameter and splint opening angle on the qualified single-seed rate when the seed-metering plate rotation speed was 30 rpm. As is evident, when the splint opening angle was fixed, the qualified rate of single-seed first increased with the increasing scoop opening diameter before decreasing. When the scoop opening diameter was constant, the qualified rate of single-seed first increased with the increasing splint opening angle before decreasing. When the scoop opening diameter was 23–25 mm, and the splint opening angle was 60–65°, the qualified rate of single-seed was shown to be higher.



(**a**) (**b**) (**c**)

Figure 13. Response surface for the interaction's influence on the qualified rate. (**a**): Response surface for the interaction between the scoop diameter and opening angle on the qualified rate. (**b**): Response surface for the interaction between rotation speed and splint opening angle on the qualified rate. (**c**): Response surface for the interaction between the scoop diameter and rotation speed on the qualified rate.

Figure 13b displays the response surface diagram of the interaction between the seed-metering plate rotation speed and splint opening angle on the qualified single-seed rate when the scoop opening diameter was 24 mm. As is evident, when the seed-metering plate rotation speed was constant, the qualified rate of single-seed first increased with the increasing splint opening angle before decreasing. When the splint opening angle was constant, the qualified rate of single-seed first increased with the increasing seed-metering plate rotation speed before decreasing. When the seed-metering plate rotation speed was 30–40 rpm, and the splint opening angle was 55–65°, the qualified rate of single-seed was higher.

Figure 13c presents the response surface diagram for the interaction between the seed-metering plate rotation speed and scoop opening diameter on the qualified single-seed rate when the splint opening angle was 60°. As is evident, when the scoop opening diameter was constant, the qualified rate of single-seed first increased with the increasing speed of the seed disc before decreasing. When the seed-metering plate rotation speed was constant, the qualified rate of single-seed first increased with the increasing scoop opening diameter before decreasing. When the seed-metering plate rotation speed was 30–40 rpm, and the scoop opening diameter was 23–25 mm, the qualified rate of single-seed was shown to be higher.

To seek the optimal combination of factors under horizontal constraints, the qualified rate, missing rate, and reply rate were used as evaluation indicators, and the model was established in combination with the factor boundary conditions. The evaluation index regression model was addressed through multi-objective optimization [23–25]. The boundary conditions for the optimization objective function can be written as follows:

$$\begin{cases} max\ Y_1 \\ min\ Y_2 \\ min\ Y_3 \\ 50^\circ \le X_1 \le 70^\circ \\ 22\ \text{mm} \le X_2 \le 26\text{mm} \\ 20\text{rpm} \le X_3 \le 40\text{rpm} \end{cases} \tag{8}$$

Multi-objective optimization was conducted using the highest qualified rate, the lowest missing rate, and the reply rate as the optimization objectives. Using Design-Expert software, we found that the optimal effect was achieved when the splint opening angle was 62.86°, the scoop opening diameter was 24.22 mm, and the seed-metering plate rotation speed was 34.19 rpm. Therefore, the qualified rate was 90.33%, the missing rate was 3.90%, and the reply rate was 5.76%.

4. Bench Verification Test

In order to confirm the reliability of the coupling simulation results, a finger clip plate garlic seed-metering device test bench was set up to test the optimized simulation results.

4.1. Test Materials and Equipment

Pizhou-sourced white garlic seeds with full grain and no skin damage were selected for the experiment. Based on the optimization simulation results and considering the processing accuracy, the seed-collecting scoop's diameter was defined as 24 mm, and the opening angle of the splint was set to 63°. The seed-metering device was virtually assembled using three-dimensional modeling software, and an interference check was conducted. The three-dimensional model of the seed-metering device was then transformed into two-dimensional drawings, and the seed feeder was processed and assembled. All parts were welded from metal sheet parts. The test bench was built on a conveyor belt, and the speed-regulating motor controlled the speed of the seed plate. Figure 14 shows the test bench.

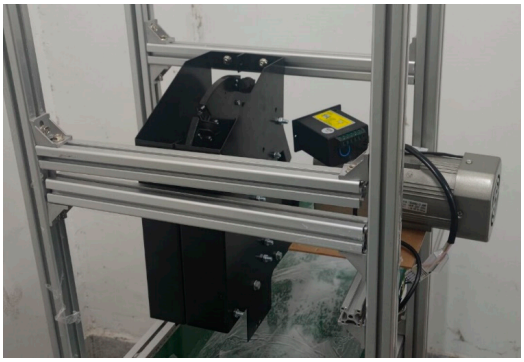


Figure 14. Finger clip plate garlic seed-metering device test bench.

In addition, the garlic planting image is shown in Figure 15. The size of garlic seeds is generally around 0.8–1.5 cm, and their shape is ovoid or oblate. The moisture content of garlic seeds ranges from 6% to 12%.



Figure 15. Garlic planting image.

4.2. Test Method

The accuracy of parameter optimization based on discrete elements and MBD simulation was verified using a bench test on the finger clip plate garlic seed-metering device. Based on the National Standard of P.R.C (GB/T 6973-2005 Test Method of Single-Seed Drills (Precision Drills) and under the same conditions as the simulations, the splint opening angle was selected at 63°, the scoop opening diameter was 24 mm, and the plate rotation speed was 34 rpm. We used the qualified rate, reply rate, and missing rate as the test indexes, and 100 seeds were selected for each test group. Three repeated tests were performed. The results were averaged [26–28].

4.3. Test Results and Analysis

The bench verification results are presented in Table 7. It is evident that under the conditions of a splint opening angle of 63°, a scoop opening diameter of 24 mm, and a plate rotation speed of 34 rpm, the average qualified rate was 90.00%, the average missing rate

was 4%, the average reply rate was 5.67%, and the error compared to the simulation test was 0.4%, indicating that the parameter optimization results are reasonable and reliable.

Table 7. Bench test results.

Project	1	2	3	Average
Qualified rate	90%	91%	89%	90.00%
Missing rate	3%	5%	5%	4.33%
Reply rate	7%	4%	6%	5.67%

5. Conclusions

A finger clip plate garlic seed-metering device was designed, and its main working principle was expounded. According to theoretical analysis of the operation of the seed-metering device, the structural design and optimization of the main working parts of the seed-metering device were carried out.

The coupling simulation of the EDEM discrete element and RecurDyn MBD software applications was adopted to establish the finger clip plate garlic seed-metering device model and garlic seed model. Through a single-factor simulation test and three-factor and five horizontal quadratic regression orthogonal rotation combination simulation test, the influence law of the splint opening angle, scoop opening diameter, and seed-metering plate rotation speed on the qualified rate of single-seed, missing rate, and reply rate of the seed-metering device were obtained. According to the results, when the splint opening angle was 62.86°, the scoop opening diameter was 24.22 mm, the plate rotation speed was 34.19 rpm, and the performance of the seed-metering device was optimal. In this case, the qualified rate of single-seed was 90.33%, the missing rate was 3.90%, and the reply rate was 5.76%.

The optimization results obtained from the simulation test were verified via a bench test, and the qualified rate of single-seed was 90.00%, the missing rate was 4.33%, and the reply rate was 5.67%, demonstrating that the parameter optimization results are reasonable and reliable.

Author Contributions: Conceptualization, Y.D., H.L., J.G., H.Y. and Y.W.; Methodology, Y.D. and J.G.; Software, Y.D. and J.G.; Validation, Y.D.; Formal analysis, Y.D. and J.G.; Investigation, J.G.; Resources, J.G.; Data curation, Y.D. and J.G.; Writing—original draft preparation, Y.D.; Writing—review and editing, Y.D., H.L., J.G., H.Y., Y.W. and D.F.; Supervision, H.L.; Funding acquisition, H.L. All authors have read and agreed to the published version of the manuscript.

Funding: This current study was financially supported by the Key special Project of National Key R & D Plan (Grant No. 2017YFD0701300) and Jiangsu Province Demonstration and Promotion of Modern Agricultural Equipment and Technology (Grant No. NJ2021-12) and Jiangsu Province Demonstration and Promotion of Modern Agricultural Equipment and Technology (Grant No. NJ2022-09) and Jiangsu middle late garlic industry cluster sub project.

Institutional Review Board Statement: Not applicable.

Data Availability Statement: The data provided in this study are available upon request from the corresponding author. For privacy reasons, these data cannot be made public.

Conflicts of Interest: The authors declare no conflict of interest.

References

1. Li, Y.D.; Niu, C.H.; Jia, S.T. Analysis of the Current Research Situation on Mechanized Garlic Seeding. *Xinjiang Agric. Mech.* **2021**, *2*, 29–33.
2. Jin, W.X.; Liu, Y.H.; Zhang, D.F. Design and test of vertical planting device for garlic. *J. Chin. Agric. Mech.* **2020**, *41*, 37–42.
3. Li, T.H.; Huang, S.H.; Niu, Z.R. Optimization and experiment of planting perpendicularity of planetary wheel garlic planter. *Trans. Chin. Soc. Agric. Eng. (Trans. Csae)* **2020**, *36*, 37–45.
4. Liu, J.Z.; Geng, A.J.; Li, X.Y. Research Status of Garlic Planting Machine Single Seed-Filling and Row. *J. Agric. Mech. Res.* **2019**, *41*, 262–268.

5. Wei, H.L.; Wang, X.Y.; Chen, J.X. Discussion on the present situation and development of mechanized garlic production in China. *J. Chin. Agric. Mech.* **2022**, *43*, 175–182.
6. Guo, H.; Cao, Y.; Song, W. Design and Simulation of a Garlic Seed Metering Mechanism. *Agriculture* **2021**, *11*, 1239. [CrossRef]
7. Wang, H.; Sun, X.; Li, H.; Fu, J.; Zeng, X.; Xu, Y.; Wang, Y.; Liu, H.; Lü, Z. Design and Parameter Optimization of a Finger Clip Plate Garlic Seed-Metering Device Based on EDEM. *Agronomy* **2022**, *12*, 1543. [CrossRef]
8. Xie, D.B.; Zhang, C.L.; Wu, X.Q. Design and Test of Garlic Seed Placer with Seed Disturbing Tooth Assisted Air Suction. *Trans. Chin. Soc. Agric. Mach.* **2022**, *53*, 47–57.
9. Wang, Y.C.; Gao, Y.C.; Tai, W.S. Design and Test of Pickup Finger Potato Precision Seed Metering Device. *Trans. Chin. Soc. Agric. Mach.* **2021**, *52*, 49–58.
10. Zhao, Q.L.; Chen, X.M.; Zhao, Y.S. Design and Test on Pickup Finger Precision Seed Metering Device for Cyperus Esculentus. *J. Jilin Agric. Univ.* **2022**, *1*, 1–9.
11. Zhou, P.; Zhao, M.Q.; Liu, F. Experimental Research on the Finger-type Corn Precision Seed-metering Device. *J. Agric. Mech. Res.* **2019**, *41*, 153–157.
12. Zhang, J.; Song, W.Y.; Cao, Y.Z.; Wang, C.; Guo, H.; Zhu, L.; Yang, F. Design and experimental research on key components of garlic seeders. *Agric. Mech. Res.* **2022**, *44*, 129–136.
13. Lai, Q.H.; Jia, G.X.; Su, W. Design and Test of Chain-spoon Type Precision Seed-metering Device for Ginseng Based on DEM-MBD Coupling. *Trans. Chin. Soc. Agric. Mach.* **2022**, *53*, 91–104.
14. Yuan, J.; Yu, J.Q. Analysis on Operational Process of Self-excited Vibrating Subsoiler Based on DEM-MBD Coupling Algorithm. *Trans. Chin. Soc. Agric. Mach.* **2020**, *51*, 17–24.
15. Hu, J.P.; Guo, K.; Zhou, C.J. Simulation and Experiment of Supplying Seeds in Box of Magnetic Precision Cylinder-seeder. *Trans. Chin. Soc. Agric. Mach.* **2014**, *45*, 61–65.
16. Xie, X.H.; Zhang, Y.; Liu, Z. Design of planting mechanism for garlic planter. *Trans. Chin. Soc. Agric. Eng. (Trans. Csae)* **2015**, *31*, 34–39.
17. Wen, E.Y.; Wu, Y.Q.; Li, T.H. Design of Traction Garlic Sowing Machine. *J. Agric. Mech. Res.* **2020**, *42*, 96–100.
18. Kang, Q.X.; Zhang, G.Z.; Zheng, L. Design and experiment of the spoon clip type seed metering device for Allium chinense. *Trans. Chin. Soc. Agric. Eng. (Trans. Csae)* **2023**, *39*, 15–25.
19. Zhang, M.H.; Jiang, Y.C.; He, S.Y. Design and experiment of the air suction wheel precision seed metering device for vegetables. *Trans. Chin. Soc. Agric. Eng. (Trans. Csae)* **2023**, *39*, 98–109.
20. Zhang, X.J.; Cheng, J.P.; Shi, Z.L. Simulation and Experiment of Seed Taking Performance of Swing-clamp Type Maize Precision Seed-metering Device. *Trans. Chin. Soc. Agric. Mach.* **2023**, *54*, 38–50.
21. Duangjit, S.; Chairat, W.; Opanasopit, P.; Rojanarata, T.; Ngawhirunpat, T. Application of Design Expert for the investigation of capsaicin-loaded microemulsions for transdermal delivery. *Pharm. Dev. Technol.* **2016**, *21*, 698–705. [CrossRef] [PubMed]
22. Peláez, J.I.; Gomez-Ruiz, J.A.; Fornari, J.; Vaccaro, G.F. Automatic identification of characteristic points related to pathologies in electrocardiograms to design expert systems. *Soft Comput.* **2019**, *23*, 4207–4219. [CrossRef]
23. Shi, S.; Liu, H.; Wei, G.J. Optimization and Experiment of Pneumatic Seed Metering Device with Guided Assistant Filling Based on EDEM-CFD. *Trans. Chin. Soc. Agric. Mach.* **2020**, *51*, 54–66.
24. Ding, L.; Yang, L.; Zhang, D.X. Design and Experiment of Seed Plate of Corn Air Suction Seed Metering Device Based on DEM-CFD. *Trans. Chin. Soc. Agric. Mach.* **2019**, *50*, 50–60.
25. Chen, H.T.; Wang, H.F.; Wang, Y.C. Design and Experiment of Three-leaf Type Air-suction Seed Meter with Automatic Clear and Replace Seeds Features for Soybean Plot Test. *Trans. Chin. Soc. Agric. Mach.* **2020**, *51*, 75–85.
26. Chen, Y.L.; Liu, Z.Q.; Han, J. Design and experiments of the flat seed-adsorbing posture adjustment mechanism for the air-suction metering device. *Trans. Chin. Soc. Agric. Eng. (Trans. Csae)* **2022**, *38*, 1–11.
27. Dong, J.X.; Gao, X.J.; Zhang, S.L. Design and Test of Maize Posture Control and Driving Precision Metering Device for High-speed Seeder. *Trans. Chin. Soc. Agric. Mach.* **2022**, *53*, 108–119.
28. Sun, X.; Li, H.; Qi, X. Performance Parameters Optimization of a Three-Row Pneumatic Precision Metering Device for Brassica chinensis. *Agronomy* **2022**, *12*, 1011. [CrossRef]

Disclaimer/Publisher's Note: The statements, opinions and data contained in all publications are solely those of the individual author(s) and contributor(s) and not of MDPI and/or the editor(s). MDPI and/or the editor(s) disclaim responsibility for any injury to people or property resulting from any ideas, methods, instructions or products referred to in the content.